Morphology and Roughness of Silver Deposit Formed by Cementation at Various Temperatures in Pure Sulfuric Acid

by **Grzegorz D. Sulka***, and **Marian Jaskuła**

Department of Physical Chemistry, Faculty of Chemistry, Jagiellonian University, Ingardena 3, 30-060 Krakow, Poland
(phone: +48-12-6632266; fax: +48-12-6340515; e-mail: sulka@chemia.uj.edu.pl)

The morphology and surface roughness of silver (Ag) deposit formed on metallic copper (Cu) by cementation conducted in a 0.5M H_2SO_4 solution was investigated at various temperatures above 25°. The influence of the presence or absence of oxygen (O_2) on Ag morphology was studied at an initial Ag^+ concentration of 20 mg/dm^3. An analysis of distribution diagrams of the surface height calculated from scanning-electron-microscope (SEM) top-view images was performed. The cementation reaction results in a non-homogeneous Ag deposit formed on the surface independently of the presence or absence of O_2 in solution. The Ag deposit covers Cu mainly with a uniform and compact layer with separated germs of predendrites, but also a huge 'fern-leaf-shaped' and 'lycopodium-twigs-shaped' dendrites appear occasionally on the surface. The presence of O_2 in the system and temperature do not affect significantly the morphology of Ag dendrite as well as a deposit formed on the smooth part of the surface. The roughness of surface with Ag cement varies with temperature only under aerobic conditions where the enhanced Cu corrosion increases the size of anodic sites. The results obtained from the surface-height-distribution diagrams constructed for anaerobic conditions showed that the reaction between Cu^+ and Ag^+ does not start in the bulk of the solution even at the highest studied temperature.

Introduction. – Cementation is an electrochemical process in which a more-noble metal ion is reduced to the solid state while a less noble metal is oxidized. The process consists of two short-circuited half-cell reactions: cathodic and anodic [1][2]. Therefore, cathodic and anodic sites are generated simultaneously on the surface of the less-noble metal when the cementation process takes place. The progress of cementation involves a constant evolution of the morphology and roughness of the reaction surface [1][2]. This is mainly responsible for difficulties connected with the mechanism determination for certain cementation processes as well as with the establishment of the correct relation between kinetics of the process and roughness of the deposit [3].

From an industrial point of view, cementation has undeniable advantages such as a pure metallic form of recovered metals, simplicity of reaction control, and low energy consumption [4]. Therefore, cementation techniques have been widely used in industry, not only for recovery or removal of various metals in hydrometallurgy [5–8], but also for purification of wastewaters bearing hazardous or poorly degradable metals [9–16]. The recovery of precious metals from dilute solutions and wastes by cementation has been used successfully for decades [17–20]. Moreover, cementation is still irreplaceable for the purification of process streams in the production of ultra-pure metals such as Zn or Cd [21–25]. Cementation of Ag^+ on Cu^0 can be described by *Eqn. 1*:

$$2\,Ag^{+} + Cu \rightarrow 2\,Ag + Cu^{2+} \quad (1)$$

In our recent papers [26–28], we reported that Ag^{+} cementation on Cu in acidic sulfate solutions as well as in a pure H_2SO_4 follows first-order kinetics. The overall kinetics of the process conducted in 0.5M H_2SO_4 is controlled by mass transfer of Ag^{+} to the reaction surface [27]. The rate enhancement of the reaction observed after the initial period of cementation (less than 10 min) carried out in the presence of 20 mg/dm^3 Ag^{+} was attributed to *ca.* 20% increase in effective surface area, independently of the presence of O_2 in the system [27]. The mechanism of the process was fully established for both anaerobic an aerobic solutions containing 0.5M H_2SO_4/0.5M $CuSO_4$ [29]. It was found that the cementation mechanism consists of two stages. The presence of O_2 in the system modifies strongly the second stage. In the first stage of the reaction, Cu^{+} ions appear in solution as a result of the reaction of Ag^{+} with Cu. The second stage of the reaction conducted under O_2-saturated conditions involves the Cu^{+} oxidation and Ag^{+} ion reduction. In O_2-free solutions, Cu^{+} ions generated in the first stage can be transferred partially into the bulk of the solution to react as follows:

$$Ag^{+} + Cu^{+} \rightarrow Cu^{2+} + Ag^{0}\ (\text{colloid}) \quad (2)$$

It should be pointed out that the progress of this side reaction (*Eqn. 2*) is directly connected with a certain value of the Cu^{+}/Ag^{+} concentration ratio to be reached during the cementation process [29]. When cementation is conducted in a 0.5M H_2SO_4/0.5M $CuSO_4$ solution under anaerobic conditions, the concentration of Cu^{+} increases strongly due to the interaction between Cu^{2+} and metallic Cu [29]. This additional concentration of Cu^{+} initiates the progress of the reaction (*Eqn. 2*) in 0.5M H_2SO_4/0.5M $CuSO_4$ [29]. In a neat H_2SO_4, the cementation does not produce enough Cu^{+} to start the progress of the reaction in bulk solution [29]. The dependence of the cementation mechanism on the composition of the solution can result in a different morphology of Ag cement formed in the presence or absence of Cu^{2+} under anaerobic conditions.

The morphology of Ag deposit was investigated before for a 0.5M H_2SO_4/0.5M $CuSO_4$ solution at 25° [29]. It was found that the presence or absence of oxygen does not affect significantly the silver morphology. Recently, the temperature effect on the morphology and surface roughness of silver deposit formed by cementation in a 0.5M H_2SO_4/0.5M $CuSO_4$ solution has been studied [30]. The evolution of surface roughness during cementation of Ag^{+} conducted in the O_2-free or O_2-saturated electrolyte containing 0.5M H_2SO_4 and 0.5M $CuSO_4$ was also investigated at two different initial concentrations of Ag^{+} [31].

The present paper is focused on the temperature influence on the morphology of Ag deposit formed by cementation in a 0.5M H_2SO_4 solution. The special emphasis is put on the analysis of the surface roughness and its relation to the mechanism of the process. Surface-height-distribution diagrams are used to obtain information on the mechanism of the process carried out in a solution containing a relatively low concentration of Ag^{+} in comparison to the reaction surface area. The nature of the cementation and electrodeposition processes are very similar due to the redox reactions taking place in both cases. Therefore, the method can be transferred to the surface-roughness analysis of various metallic deposits obtained by electrodeposition.

Experimental. – All chemical reagents were of anal. grade. Four times distilled H_2O was used to prepare all solns. Experiments were conducted in a rotating cylinder system described previously [26]. The rotating steel cylinder had a working surface area of 27.5 cm^2. Before each run, the rotating cylinder was carefully pretreated by immersion in HNO_3/H_2O 1:1 (*v*/*v*), followed by rinsing with H_2O and degreasing with MeOH. Then, the steel cylinder was covered with a fresh 24-μm-thick layer of Cu by electrolysis at a const. current of 36.4 mA/cm^2 for 30 min at 20° in an electrolyte containing 0.5M H_2SO_4 and 0.5M $CuSO_4$. The deposited Cu layer was electropolished at const. current (72.7 mA/cm^2) for 40 s at 20° in H_3PO_4/H_2O 3:1 (*v*/*v*) and finally chemically polished for 1 min in 0.5M H_2SO_4 solution at 20°. After polishing, the cylinder was rinsed with H_2O, dried in air at r.t., and used for the cementation test.

The electrolyte used for cementation was 0.5M H_2SO_4 containing 20 mg/dm^3 of Ag^+ (Ag_2SO_4). The initial concentration of Ag^+ was determined before the experiment by atomic-absorption spectroscopy (AAS). The electrolyte used in each experiment had a volume of 0.2 dm^3, and was stirred at 500 r.p.m. The cementation tests were carried out between 25° and 55°. Before each run, the electrolyte in the cell was purged by bubbling with high-purity Ar gas or high-purity O_2 for 20 min. The O_2-free or O_2-saturated atmosphere was maintained throughout the whole process by passing Ar or O_2. Experiments conducted in the presence or absence of O_2 are referred to as *aerobic* and *anaerobic*, resp. The duration of each experiment was 60 min. After each run, the Cu layer with cemented Ag was rinsed carefully and dried at r.t., then cut and separated from the cylinder. Two samples of the Cu sheet with cemented Ag were taken, dissolved in hot HNO_3/H_2O 1:1, and analyzed for the Ag content by AAS. The surface area of each sample taken for AAS analysis was about 3.5 cm^2. For each cementation test, the surface of two samples of the Cu sheet with cemented Ag was observed with a *Hitachi S-4700* scanning electron microscope (SEM). SEM Images were analyzed with the scanning-probe image processor WSxM 3.0 Beta [32].

Results and Discussion. – The morphology and roughness of Ag deposit formed by the cementation was investigated under both O_2-free and O_2-saturated solutions containing 20 mg/dm^3 Ag^+ at 25° to 55°. A typical low-magnification SEM top-view image of the Cu surface with cemented Ag (*Fig. 1*) showed a highly non-homogeneous Ag deposit. Most of the surface looked rather smooth and flat. Germs of pre-dendrites as well as a huge single dendrite were occasionally visible on the surface. Similar SEM images with a single dendrite were observed for other temperatures, independently of the presence or absence of O_2 in the system. These results suggest a similar Ag coverage of the Cu surface for all temperatures. Indeed, the percentage of cemented silver found on the copper surface after the cementation process was almost the same for all temperatures, both under aerobic and anaerobic conditions.

The *Table* shows the average percentage of cemented Ag in comparison to the initial Ag content (determined by AAS) for O_2-free and O_2-saturated solutions. The percentage of cemented Ag was found to oscillate between 78 and 82% in all cases. These data are fully consistent with the previously presented kinetics curves [27], where both methods used for the determination of the Ag^+ concentration in solution led to the same result and, consequently, do not reflect the progress of the reaction (*Eqn. 2*) in O_2-free solution, even at the highest studied temperature [27][29]. It was found that the reaction starts in bulk solution only after achieving a certain threshold of the Cu^+/Ag^+ concentration ratio [29]. Therefore, the rate enhancement observed in the latter stage of the process taking place in solution, at an initial Ag^+ concentration of 20 mg/dm^3, is closely related to the increase of the effective surface area of the cathodic sites and formation of dendrites on the surface [27].

To better examine the surface roughness of smooth parts of the Ag cement formed on Cu, higher-magnification SEM top-view images were taken and analyzed. The ana-

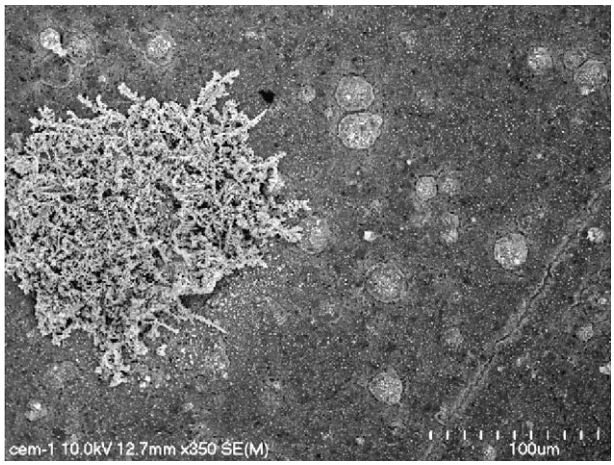

Fig. 1. *SEM Top-view image of the Cu surface with Ag deposit formed by cementation in aerobic solution containing 20 mg/dm³ Ag^+ at 35°.* In 0.5M H_2SO_4 electrolyte for 60 min.

Table. *Average Percentage of Cemented Ag on Cu under Different Cementation Conditions*

T [°]	Anaerobic			Aerobic		
	n[a])	Ag [%][b])	SD [%][c])	*n*	Ag [%]	SD [%]
25	3	77.7	5.0	3	78.4	1.8
35	3	82.0	2.9	3	81.7	1.8
55	3	79.8	1.8	3	80.3	1.8

[a]) Number of independent cementation experiments. [b]) Determined by atomic absorption spectroscopy (AAS). [c]) Standard deviation.

lyzed surface area of samples was *ca.* 500 μm². *Fig. 2* shows SEM top-view images of the Cu surface with cemented Ag, together with their surface-height-distribution diagrams at various temperatures in anaerobic solution containing 20 mg/dm³ Ag^+. A semi-quantitative analysis of the surface-height distribution was performed. The peak width at half peak height, $W_{1/2}$, was measured for all distribution diagrams (*Fig. 2*).

At the beginning of the process, Ag covers uniformly the Cu surface with tiny Ag crystals [31]. When the surface is covered compactly, the Ag deposition starts from protrusions existing on the surface. As a result of the reaction progress, some germs of pre-dendrites appear on the surface. Such germs of pre-dendrites are visible in SEM images as white spots. At the same time, anodic sites are formed on the surface and develop their working surface area mainly in the Cu material just under the deposited Ag, with formation of deep cavities [29]. Anodic sites are exhibited in SEM images as a net of dark cracks. With increasing temperature, the rate of the cementation process increases, and anodic sites are regularly spread over the reaction surface [30]. As a result, at the highest temperature, the dense net of cracks is visible in *Fig. 2,c*. The distribution diagrams in *Fig. 2,a* and *2,b* do not vary significantly (similar $W_{1/2}$ values) showing relatively narrow and intense peaks. The peak width $W_{1/2}$ increases slightly

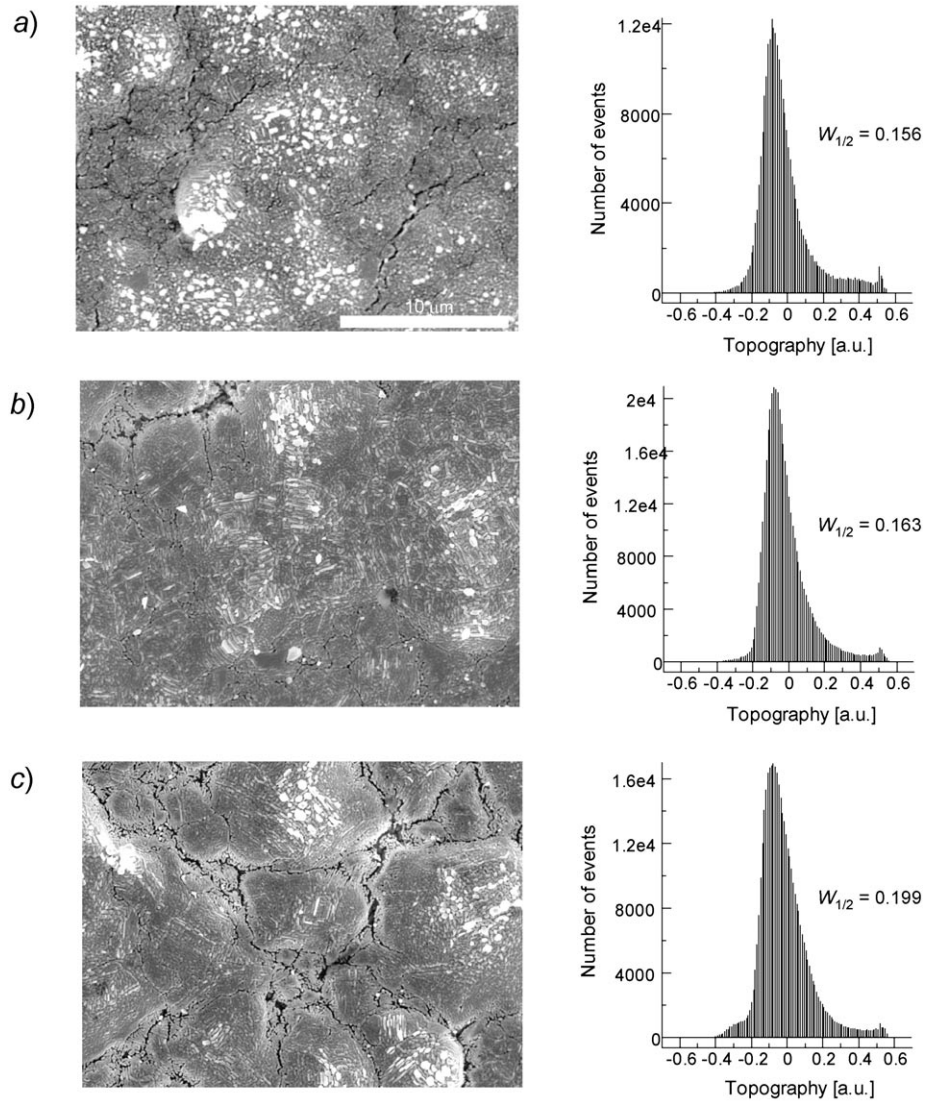

Fig. 2. *SEM Top-view images and distribution diagrams of the surface height for an anaerobic solution containing 20 mg/dm³ Ag^+ at 25°* (a), *35°* (b), *and 55°* (c). In 0.5M H_2SO_4 electrolyte for 60 min. The analyzed surface area was *ca.* 500 µm².

when the temperature increases to 55°. The wide range of surface heights in the positive region (protruding) of all diagrams presented in *Fig. 2* corresponds closely with predendrites visible in SEM images. At the highest studied temperature, the surface-height-distribution histogram shows a small difference in the negative range of surface heights in comparison to the others presented in *Fig. 2,a* and *2,b*. The wider range of negative heights in *Fig. 2,c* exhibits a denser net of anodic sites and is directly respon-

sible for the observed increase in $W_{1/2}$. SEM Top-view images taken at various temperatures and, especially, surface-height-distribution diagrams can indicate formation of cathodic and anodic sites on the surface in the cementation process.

SEM top-view images of the Cu surface with Ag deposit formed at various temperatures in O_2-saturated solution containing 20 mg/dm^3 Ag^+ are presented in *Fig. 3*, together with the corresponding surface-height-distribution diagrams calculated for a surface area of *ca.* 500 μm^2. Similar as for the O_2-free solution, some germs of dendrites are visible on the reaction surface. In contrast to the O_2-free solution, temperature has a great impact on the morphology of Ag deposit when O_2 is present in the system. As can be expected for aerobic conditions, especially at the highest temperature, Cu corrosion is strongly enhanced. As a result, the anodic sites are spread uniformly over the reaction surface and form a very dense net of broad cracks (*Fig. 3*, *c*).

Increasing temperature modifies the roughness of the Ag deposit formed in the presence of O_2, as clearly reflected in the distribution diagrams. With increasing temperature, a broadening of peaks occurs ($W_{1/2}$ increases) as a result of formation and expansion of the anodic sites on the surface. The presence of these anodic sites is especially pronounced at 55°, with a very wide range of negative values in the diagram heights (*Fig. 3*, *c*). It should be pointed out that the percentage of cemented Ag remains almost constant for the studied range of temperatures (*Table*) and cannot affect the surface-height-distribution diagrams. For O_2-saturated solutions, due to enhanced Cu corrosion, the surface-height-distribution diagrams show broader peaks than those found under O_2-free conditions ($W_{1/2}$ in *Fig. 2 vs. Fig. 3*).

As mentioned before, the cementation process can promote formation of huge Ag dendrites. Some parts of the surface are covered with tiny Ag crystals, but others are occupied by 'fern-leaf-shaped' and 'lycopodium-twigs-shaped' dendrites. *Fig. 4* shows SEM images of such Ag dendrites. Their morphology does not change significantly with increasing temperature. Moreover, the presence or absence of O_2 in the system does not modified strongly the 'fern leaf-shaped' dendrites. The only (small) difference can be observed for the O_2-saturated solution at temperatures above 25° (*Fig. 4*, *d* and *4*, *f*): the Ag deposit seems to be a bit denser and the 'twigs' thicker. To further illustrate the possible influence of the presence of O_2 on the morphology of dendrites, higher-magnification SEM images are presented in *Fig. 5*. There is no observable difference in the morphology of Ag dendrites formed at 55° under anaerobic or aerobic conditions. The 'fern-leaf-shaped' dendrites seems to be covered with fine granular Ag crystals sticking out from their surface independently of the presence or absence of O_2.

Higher-magnification SEM top-view images of the surface with Ag deposited at 55° under anaerobic and aerobic conditions are shown in *Fig. 6*. The images have been taken from a flat part of the surface where no dendrite formation was observed. Similar SEM images of the reaction surface were taken for other studied temperatures. Here, the Ag deposit covers Cu with a uniform Ag layer. Moreover, the size of the Ag crystals is independent of the presence or absence of O_2 in the system. Previously, it was found that the adherence of the Ag deposit formed in the O_2-free solution was a bit better than under aerobic conditions [29]. This apparent difference can be attributed to the evident presence of the anodic site in the close neighbourhood of the examined deposit formed in the presence of O_2. This detailed examination of Ag crystals formed at var-

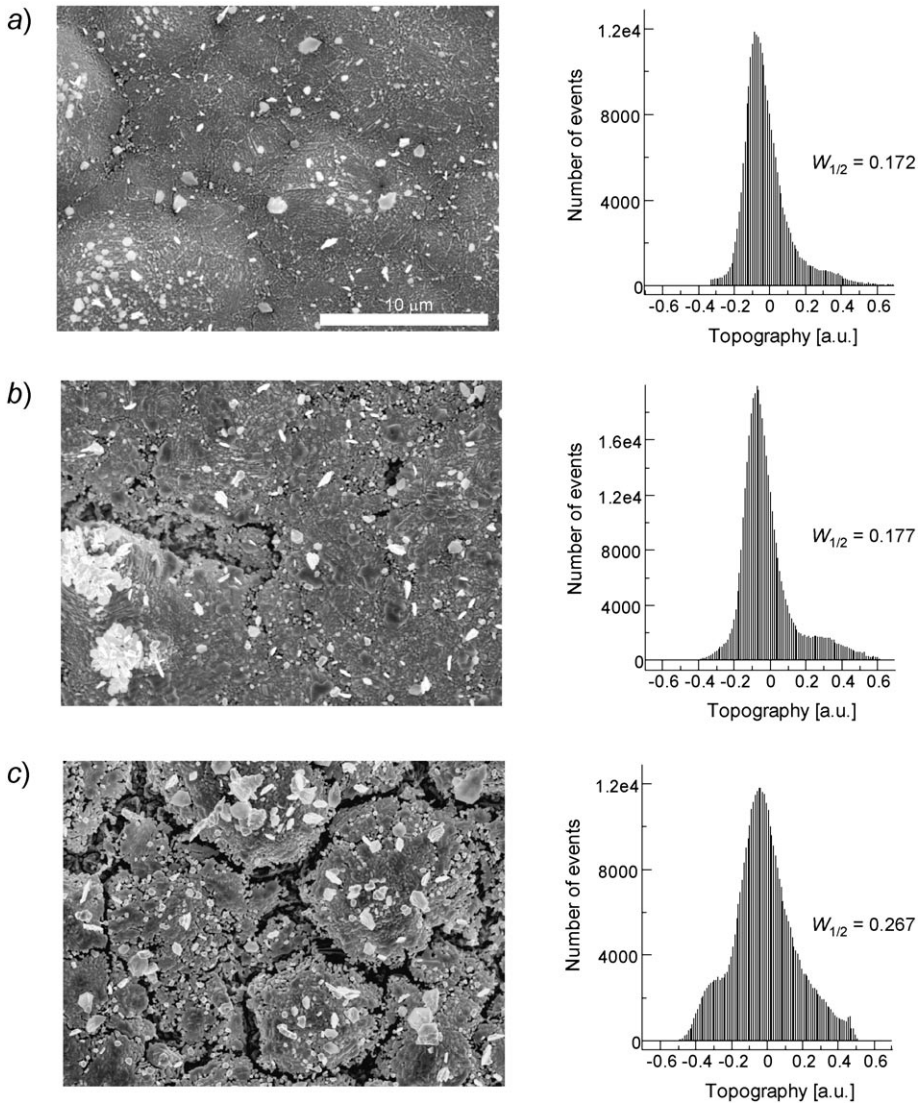

Fig. 3. *SEM Top-view images and distribution diagrams of the surface height for an aerobic solution containing 20 mg/dm³ Ag^+ at 25°* (a), *35°* (b), *and 55°* (c). In 0.5M H_2SO_4 electrolyte for 60 min. The analyzed surface area was *ca.* 500 μm².

ious temperatures shows that the presence of O_2 as well as temperature do not influence significantly the morphology of Ag deposit.

Conclusions. – The cementation process conducted in 0.5M H_2SO_4 solution containing 20 mg/dm³ Ag^+ leads to formation non-homogeneous Ag deposit on the surface, independently of the presence or absence of O_2 in the system. Parts of the surface

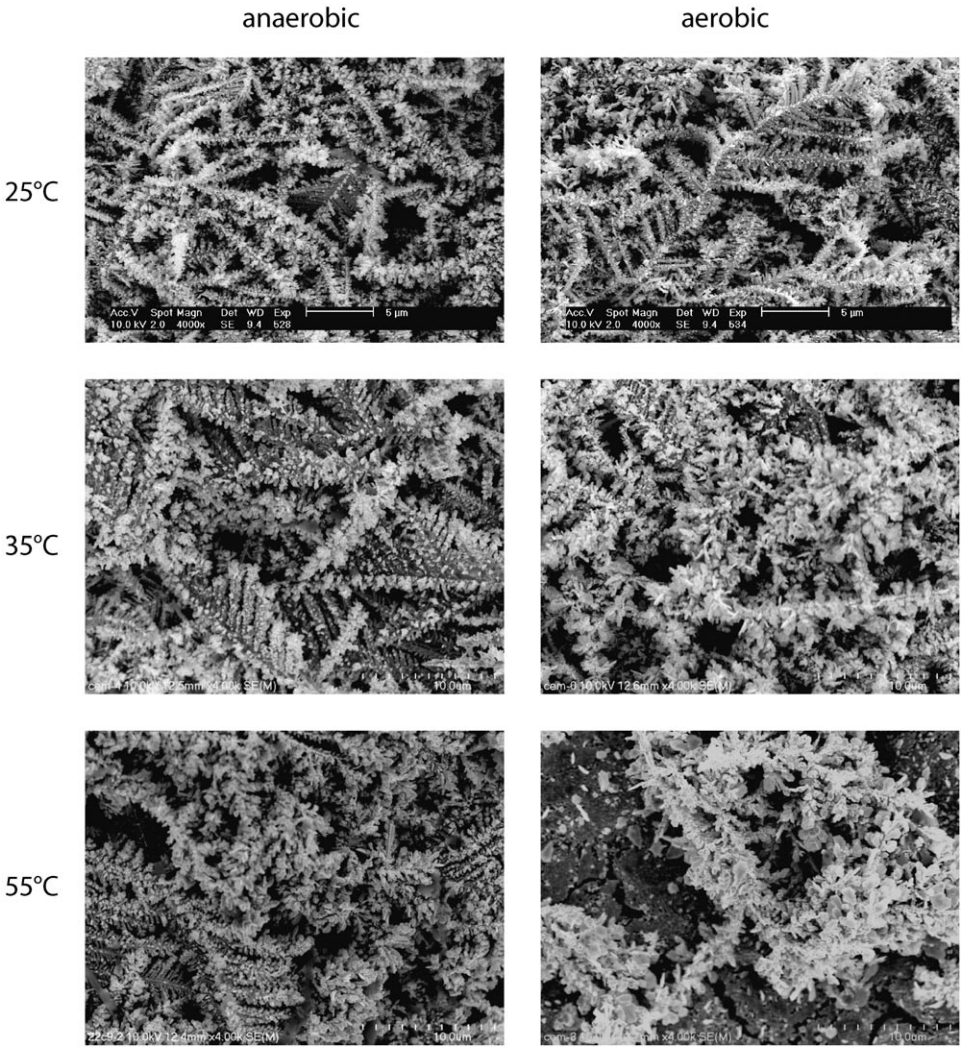

Fig. 4. *SEM Top-view images of Ag dendrites formed at various temperatures in anaerobic and aerobic solutions containing 20 mg/dm³ Ag^+.* In 0.5M H_2SO_4 electrolyte for 60 min.

are covered with a relatively smooth Ag deposit with germs of pre-dendrites, but others exhibits huge 'fern leaf-shaped' and 'lycopodium-twigs-shaped' dendrites. The presence of O_2 and temperature do not affect significantly the morphology of Ag dendrites as well as the deposit formed on the smooth part of the surface.

For O_2-free solutions, the surface-height-distribution diagrams calculated at various temperatures for the part of the surface where Ag deposit exhibits a relatively tight, well-adhered structure, with some separate germs of pre-dendrites, show no difference in surface roughness. The roughness of the deposit increases significantly with increasing temperature in the case when O_2 is present in solution. In the presence of O_2,

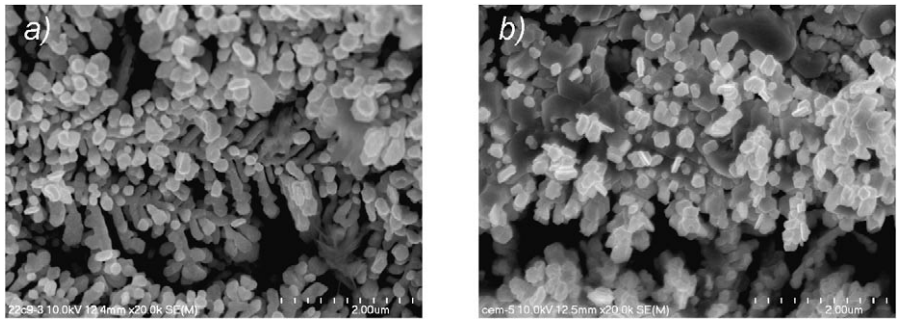

Fig. 5. *High-magnification SEM top-view images of Ag dendrites formed at 55° in anaerobic* (a) *and aerobic* (b) *solutions containing 20 mg/dm³ Ag^+*. In 0.5M H_2SO_4 electrolyte for 60 min.

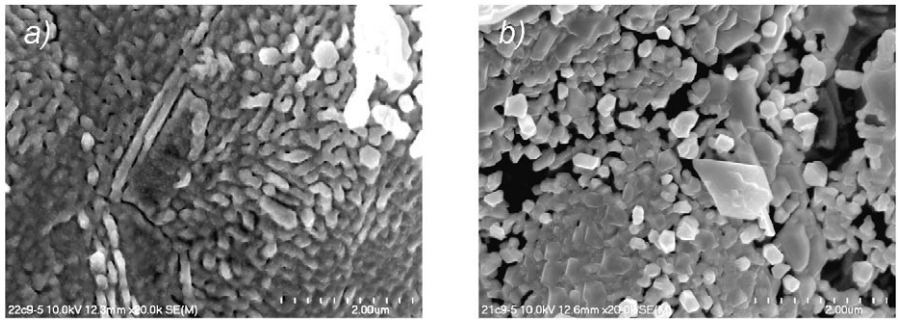

Fig. 6. *High-magnification SEM top-view images of the smooth and tight Ag deposit formed at 55° in anaerobic* (a) *and aerobic* (b) *solutions containing 20 mg/dm³ Ag^+*. In 0.5M H_2SO_4 electrolyte for 60 min.

enhanced Cu corrosion leads to the formation and expansion of anodic sites over the reaction surface, which results in broadening of peaks in the surface-height-distribution histograms. As a result, various negative heights appear in the diagrams. These analyses are fully consistent with the kinetics data and mechanism of the process [27][29]. For the O_2-free solution, the optional progress of the reaction (*Eqn. 2*) especially at elevated temperature 55° [29], should result in a flattening effect of the surface roughness [30]. The analysis of height-distribution diagrams and the percentage of cemented Ag does not indicate the progress of the reaction. The surface-height-distribution diagrams show that the competitive reaction between Ag^+ and Cu^+ does not start in anaerobic solution containing 0.5M H_2SO_4, not even at the highest studied temperature. Nevertheless, analysis of surface-height-distribution diagrams provides useful information about the evolution of anodic sites during cementation.

We kindly acknowledge the Laboratory of Field Emission Scanning Electron Microscopy and Microanalysis at the Institute of Geological Sciences, Jagiellonian University (Poland), were SEM imaging has been performed.

REFERENCES

[1] M. E. Wadsworth, *Trans. Met. Soc. AIME* **1969**, *245*, 1381.
[2] J. D. Miller, *Metall. Treatises* **1981**, 95.
[3] G. P. Power, I. M. Ritchie, in 'Modern Aspect of Electrochemistry', Eds. B. E. Conway, J. O'M. Bockris, Plenum Press, New York 1975, Vol. 11, pp. 199–250.
[4] R. D. Agrawal, *J. Mines, Metals Fuels* **1988**, March, 138.
[5] M. El-Batouti, *J. Colloid Interface Sci.* **2005**, *283*, 123.
[6] A. A. Mubarak, A. H. El-Shazly, A. H. Konsowa, *Desalination* **2004**, *167*, 127.
[7] M.-S. Lee, J.-G. Ahn, J.-W. Ahn, *Hydrometallurgy* **2003**, *70*, 23.
[8] F. A. López, M. I. Martín, C. Pérez, A. López-Delgado, F. J. Alguacil, *Water Res.* **2003**, *37*, 3883.
[9] M. El-Batouti, *Anti-Corrosion Meth. Mater.* **2005**, *52*, 42.
[10] A. Dib, L. Makhloufi, *Chem. Eng. Process.* **2004**, *43*, 1265.
[11] K. Lee, I. Lee, *J. Ind. Eng. Chem.* **2004**, *10*, 196.
[12] S. A. Nosier, *Chem. Biochem. Eng. Q.* **2003**, *17*, 219.
[13] Y.-S. Shen, Y. Ku, M.-H. Wu, *Sep. Sci. Technol.* **2003**, *38*, 3513.
[14] Y. Ku, M.-H. Wu, Y.-S. Shen, *Waste Manage.* **2002**, *22*, 721.
[15] T. Bigg, S. J. Judd, *Environ. Technol.* **2000**, *21*, 661.
[16] S. A. Nosier, S. A. Sallam, *Sep. Purif. Technol.* **2000**, *18*, 93.
[17] J. D. Miller, R. Y. Wan, J. R. Parga, in 'Precious and Rare Metal Technologies', Eds. A. E. Torma, I. H. Gundiler, Elsevier, Amsterdam, Oxford, New York, Tokyo, 1989, pp. 281–290.
[18] C. A. Fleming, *Hydrometallurgy* **1992**, *30*, 127.
[19] B. Dönmez, F. Sevim, S. Çolak, *Chem. Eng. Technol.* **2001**, *24*, 91.
[20] S. H. Castro, M. Sánchez, *J. Cleaner Prod.* **2003**, *11*, 207.
[21] B. B. Boyanov, V. V. Konareva, N. K. Kolev, *Hydrometallurgy* **2004**, *73*, 163.
[22] J. Näsi, *Hydrometallurgy* **2004**, *73*, 123.
[23] T. M. Dreher, A. Nelson, G. P. Demopoulos, D. Filippou, *Hydrometallurgy* **2001**, *60*, 105.
[24] D. Stanojević, B. Nikolić, M. Todorović, *Hydrometallurgy* **2000**, *54*, 151.
[25] A. Nelson, W. Wang, G. P. Demopoulos, G. Houlachi, *Min. Pro. Ext. Met. Rev.* **2000**, *20*, 325.
[26] G. D. Sulka, M. Jaskuła, *Hydrometallurgy* **2002**, *64*, 13.
[27] G. D. Sulka, M. Jaskuła, *Hydrometallurgy* **2003**, *70*, 185.
[28] G. D. Sulka, M. Jaskuła, *Hydrometallurgy* **2005**, *77*, 131.
[29] G. D. Sulka, M. Jaskuła, *Hydrometallurgy* **2004**, *72*, 93.
[30] G. D. Sulka, M. Jaskuła, *Helv. Chim. Acta* **2006**, *89*, 427.
[31] G. D. Sulka, M. Jaskuła, *Helv. Chim. Acta* **2006**, *89*, 902.
[32] WSxM, Nanotec Electronica SL, Spain (http://www.nanotec.es).

Received July 10, 2006